

Propagating Spiral Waves Obtained in a Catalyst-Immobilized Gel Membrane by the Belousov-Zhabotinsky Reaction System

Bong Seong Kim, Eun Ae Jo, C. Basavaraja, and Do Sung Huh*

Department of Chemistry and Institute of Basic Science, Inje University, Gimhae, Kyungnam 621-749, Korea

*E-mail: chemhds@inje.ac.kr

Received March 11, 2010, Accepted May 15, 2010

The formation of diverse spiral waves was studied in a polyacrylamide gel membrane with ruthenium(4-vinyl-4'-methyl-2,2'-bipyridine)bis(2,2'-bipyridine)bis(hexafluorophosphate) by a gas-free Belousov-Zhabotinsky (BZ) reaction system containing 1,4-cyclohexanedione (1,4-CHD). The gel membrane was found to be receptive for observing propagating waves since a clearer wave-train is obtained during a long reaction time without any disturbance from the immobilized metal catalyst which can be dissolved into the highly acidic solution of the BZ system. The distinctive waves in the system basically depend on both BrO₃ and 1,4-CHD in the initial phase, and are influenced by the intensity of illumination of visible light.

Key Words: Spiral waves, Gel membrane, BZ reaction, Illumination

Introduction

Chemical wave formation is one of the central problems in the study of modern macroscopic reaction kinetics.¹⁻⁷ Studies on the Belousov-Zhabotinsky (BZ) reaction and its family, which are normally understood as catalytic oxidation and bromination of organic acids, were thoroughly conducted to understand nonlinear phenomena in both animate and inanimate systems.⁸ Reaction-diffusion (RD) patterns in the BZ reactions have likewise been studied for homogeneous and inhomogeneous reaction mixtures.^{9,10} Small-sized physico-chemical systems as well as biological tissues are found to self-organize into coherent spatio-temporal activity. These biological systems include heart muscle, aggregating cells in the slime mold *Dictyostelium discoideum*, calcium waves in *Xenopus* oocytes, and spreading depression in chicken retina.¹¹⁻¹³ For studies on the chemical wave propagation in inhomogeneous conditions, various systems using a catalyst-binding matrix, such as silica gel, polysulfone membranes and ion-exchange resin, have also been investigated.¹⁴⁻¹⁹ The BZ reaction with ferroin catalyst immobilized on beads of cation-exchange resin offers a convenient experimental system for studying inhomogeneous excitable mediums. Maselko *et al.* studied regular and irregular spatial wave behaviors in BZ reaction systems with ferroin catalyst of varying cation-exchange resin sizes and concentrations of the reaction solution.²⁰ Meanwhile, Yoshikawa *et al.* reported how the oscillating frequency in a single particle relies on bead size with a similar experimental system to that presented in the study of Maselko *et al.*²¹

Kurin-Csörgei, Szalai, and Körös reported pattern formation in CO₂ gas free bromate-1,4-cyclohexanedione-ferroin oscillating reaction system.²² The absence of gas production makes this system an attractive candidate for investigating chemical wave formation.²²⁻²⁶ Another interesting and dynamic feature of bromate-1,4-cyclohexanedione-ferroin oscillating reaction is its complicated response to illumination. Kurin-Csörgei *et al.* reported that illumination with moderate intensity results in an increase in frequency of oscillations and wave speed in bro-

mate-1,4-cyclohexanedione-ferroin reaction; however, stronger illumination eliminates wave activity.²³

Huh *et al.* previously reported a characteristic wave propagation in the bubble-free BZ reaction system using 1,4-cyclohexanedione with ferroin catalyst that was immobilized in a cation-exchange resin.¹⁴ In the reaction system, a new kind of wave is induced spontaneously under a long time lag after the disappearance of the initially induced wave. This is an unusual phenomenon that has not been obtained in the BZ reaction using malonic acid, wherein an initially induced wave propagates continuously without a break for a new wave. Huh *et al.* also reported the influence of visible light on the formation of characteristic wave behaviors obtained in a bromate-1,4-cyclohexanedione-ferroin reaction system, which was used to uncover the chemical reaction mechanism for the unusual wave behavior in the bubble free system.²⁷ However, there are unchanged denunciations for the formation of the revival wave whether it is induced by a pure chemical process or by another effect such as reaction medium. It has not been well studied even though we admit that a discrete nature of cation-exchange resin that can act as an initiating site of a new wave.

Differently from resin beads, polymer gel provides a cross-linked polymer network. It is swollen in solvent, and many kinds of polymeric gels that undergo abrupt volume change in response to external stimuli, such as a change in solvent composition,²⁸ temperature,^{29,30} pH,³¹ and electric field,³² have been developed over the last two decades. Gels consisting of *N*-isopropylacrylamide (NIPAAm), which swell by cooling and deswell by heating, have been widely studied.^{33,34} Yoshida *et al.* introduced a novel self-oscillating gel that autonomously swells and de-swells periodically without any external stimuli by coupling a gel with the oscillating dynamics of the BZ reaction.^{35,36} This is prepared using a copolymer gel of a temperature-responsive NIPAAm in which Ru(bpy)₃²⁺ is covalently bonded to the polymer chain, and then acts as a catalyst of the BZ reaction.³⁷ Such self-oscillating behavior may create new possibilities for polymer gels as new functional materials demonstrat-

ing rhythmical motion or self-beating. Similarly, the gel membrane can be used as an effective reaction medium for RD pattern formation in the BZ systems since the discrete nature in the cation-exchange resin system is relaxed by the homogeneous thin gel membrane.

Due to the easy implementation of external perturbation, photosensitive reaction-diffusion media have been employed frequently in an effort to understand the interactions between intrinsic dynamics and external perturbations.³⁸⁻⁴⁵ Among these studies, the photosensitive BZ reaction has been primarily employed as the model system, resulting in the oxidation and bromination of malonic acid by acidic bromate present in a metal catalyst, $\text{Ru}(\text{bpy})_3^{2+}$. For example, Vanag *et al.* recently showed multi-phase oscillatory cluster pattern formation in a light-driven BZ medium.^{40,41} Showalter and his group employed spatio-temporal random, forcing to manifest the constructive role of noise in sub-excitable BZ media.^{42,43} They reported the presence of spatiotemporal stochastic resonance in a noisy BZ medium, in which the presence of random variation in external light intensity significantly improved the propagation of wave segments. Müller *et al.* used illumination to create and manipulate the dynamics of spiral waves, including the formation of multi-armed spirals and feedback perturbations that govern spiral drift.⁴⁵

Here, we report the emergence of diverse spiral waves in a modified BZ reaction system adopting 1,4-CHD instead of malonic acid sustained in a catalyst-immobilized gel membrane. The use of catalyst-immobilized gel membrane provides several advantages compared to the widely used ferroin loaded cation-exchange resin system. The disturbance in wave propagation induced from the secession of the immobilized metal catalyst, which has been set into the highly acidic aqueous solution, is eliminated because the metal catalyst has been covalently bonded in the gel membrane system. In addition, a discrete nature of the inhomogeneous medium of resin beads, which can serve as an initiating point to trigger a new wave, can also be relaxed in the gel membrane system. The dependence of the complex patterns on the reaction conditions is summarized in the phase diagram spanned by $[\text{BrO}_3^-]_0$ and $[1,4\text{-CHD}]_0$, wherein subscript 0 means that the concentrations are in the initial phase. The effect of visible light illumination on the propagation of wave pattern in the gel membrane system was also studied by the variation of the intensity of the illumination.

Experimental

Materials. The metal catalyst monomer, (4-vinyl-4'-methyl-2,2'-bipyridine) bis (2,2'-bipyridine) bis (hexafluorophosphate) (hereinafter abbreviated as $\text{Ru}(\text{bpy})_3^{2+}$ monomer), was purchased from Fuji Molecular Planning Ltd. (Japan). Acrylamide (AAm) as a backbone monomer for the gel membrane, *N,N'*-methylenebisacrylamide (cross-linker), ammonium persulfate (APS, initiator), and *N,N,N',N'*-teramethylethylenediamine (accelerating agent), were purchased from Sigma Aldrich. All reagents were used without further purification. Working solutions for the BZ reaction were prepared from the stock solutions of 0.6 M 1,4-cyclohexanedione (Fluka, 98%, 1,4-CHD), 0.75 M sodium bromate (Aldrich, 99%, NaBrO_3), all of which were dissolved in deionized water, and 4 M nitric acid (Aldrich, 98%,

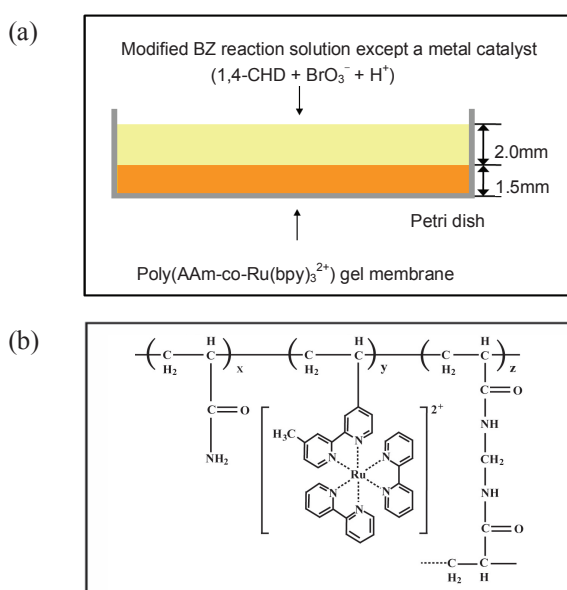


Figure 1. (a) Reaction scheme of the gel membrane, and (b) the structure of Poly(AAm-co- $\text{Ru}(\text{bpy})_3^{2+}$) gel membrane.

HNO_3) diluted with deionized water.

Synthesis of gel membrane and wave propagation. The concentration of the $\text{Ru}(\text{bpy})_3^{2+}$ monomer was fixed to the appropriate concentration: $[\text{Ru}(\text{bpy})_3^{2+}]_0 = 1.75 \text{ mM}$ in all experiments. Figure 1(a) shows the scheme of the reaction system and Figure 1(b) shows the chemical structure of the gel membrane. The poly(AAm-co- $\text{Ru}(\text{bpy})_3^{2+}$) gel membrane was synthesized by the method of Yoshida *et al.*^{35,36} by dissolving 1.5 g of acrylamide, 7.87 mg of $\text{Ru}(\text{bpy})_3^{2+}$ monomer, 0.02 g of *N,N'*-methylenebisacrylamide, and 0.02 g of ammonium persulfate in 5 ml water. After complete dissolution, 5 μL of *N,N,N',N'*-teramethylethylenediamine was added as an accelerating agent for the formation of a homogeneous thin gel membrane. This mixture was stirred and immediately transferred to a Petri dish, whose diameter was 3.5 cm. The gel membrane was washed with deionized water to remove unreacted monomers and chemicals. The Petri dish was maintained at room temperature of $20.0 \pm 0.5 \text{ }^\circ\text{C}$.

All experiments were monitored using a CCD camera (Sony, SSC-370) equipped with a zoom lens (Niko, 1.4X). The CCD camera was connected to a personal computer running a frame grabber (Flash Point, Optimus 6.1). A halogen lamp (Microtech, Model No. DLS-100HD, 100 W) was used as the light source for illumination. The light was guided to the Petri dish using an optical fiber of 5 mm in diameter. All illuminations were applied through the top of the Petri dish. The surface light intensity was controlled qualitatively between 0 and 50 mW cm^{-2} . Single pulse light perturbations were employed throughout this study. Consequently, appropriate concentrations of BZ solution, except the metal catalyst, were poured into the dish to observe wave propagation. The reaction solution of $[\text{BrO}_3^-]_0 = 0.15 \text{ M}$, $[\text{H}^+]_0 = 1.0 \text{ M}$, and $[1,4\text{-CHD}]_0 = 0.10 \text{ M}$ was used as a standard. The thicknesses of the gel membrane were controlled as constant $1.5 \pm 0.2 \text{ mm}$. The solution layer for the BZ reaction was taken as $2.0 \pm 0.3 \text{ mm}$.

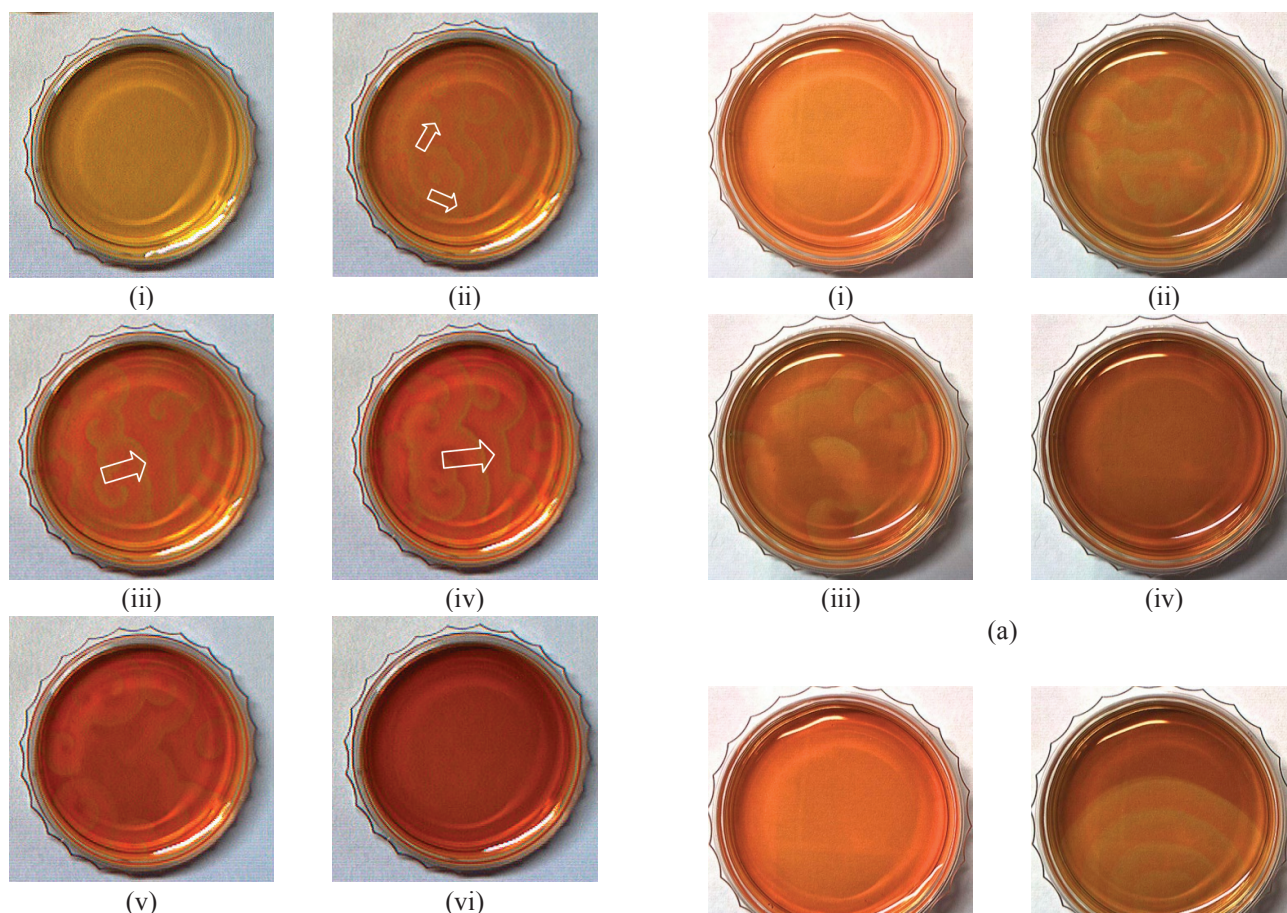


Figure 2. Typical propagation of oxidation waves on the gel membrane with a spiral wave as a folding spiral style in a modified BZ reaction system at $[\text{BrO}_3^-]_0 = 0.15 \text{ M}$, $[\text{H}^+]_0 = 1.0 \text{ M}$, $[\text{1,4-CHD}]_0 = 0.10 \text{ M}$, and $[\text{Ru}(\text{bpy})_3^{2+}]_0 = 1.75 \text{ mM}$ taken as a standard: $t =$ (i) 306, (ii) 318, (iii) 324, (iv) 357, (v) 401, and (vi) 423 min.

Results and Discussion

Distinctive propagation of the wave pattern in the gel membrane. The gel membrane itself formed a homogeneous uniform film on the bottom of the reaction Petri dish for the reaction-diffusion pattern by the BZ reaction mixture consisted of 1,4-CHD, bromate, and sulfuric acid solution without any other metal catalyst. The color of the gel membrane was changed by pouring the reaction mixture from orange to green by oxidizing the metal catalyst of Ru^{2+} monomer ion. The initial color of the membrane after mixing the BZ reaction mixture slowly changed to green, compared to the ferroin catalyst which was immobilized on the cation-exchange resin.²⁷ This shows that the gel membrane system sustaining the metal catalyst by the cross-linking network has a slower sensitivity to the oxidation and reduction change by the reaction of the environmental solution. Figure 2 shows typical spiral waves obtained in the gel membrane under the standard conditions of $[\text{BrO}_3^-]_0 = 0.15 \text{ M}$, $[\text{H}^+]_0 = 1.0 \text{ M}$, and $[\text{1,4-CHD}]_0 = 0.10 \text{ M}$. The variation of concentration was done on the basis of this standard condition. A long period of induction time was necessary for a pattern formation in this gel system as shown in step (i). After about 300 min, segmented spiral waves were formed spontaneously in

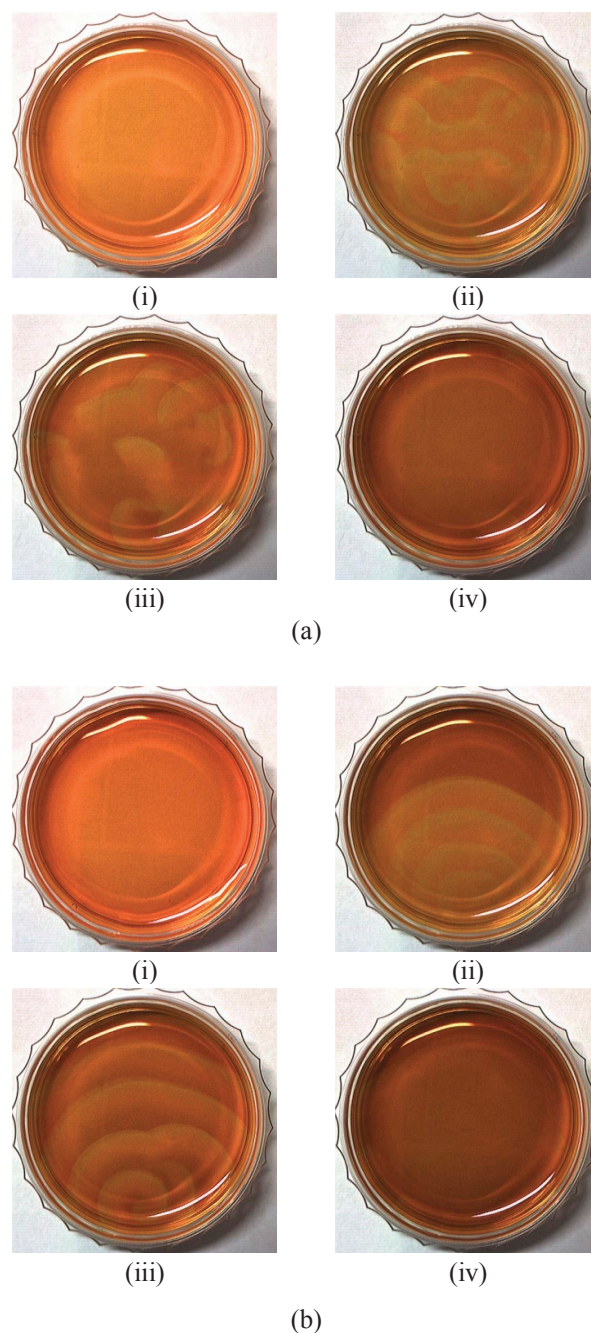


Figure 3. The wave propagating patterns in the gel membrane at different $[\text{BrO}_3^-]_0$. The concentration of the other reactants was fixed at a standard condition similar to Figure 2. Pattern (a) shows the images obtained at $[\text{BrO}_3^-]_0 = 0.125 \text{ M}$, $t =$ (i) 300, (ii) 360, (iii) 390, and (iv) 420 min, respectively. Pattern (b) shows the images at $[\text{BrO}_3^-]_0 = 0.175 \text{ M}$, $t =$ (i) 321, (ii) 408, (iii) 428, and (iv) 470 min, respectively.

the gel membrane, showing a folded pattern dependent on the initial concentration of the reactants as shown in steps (ii) to (vi). The induction time for the wave initiation of ~ 300 min was very long compared to the system using ferroin immobilized cation-exchange resin, wherein the initial wave was induced after ~ 30 min upon pouring of the reaction mixture.²⁷ It can be interpreted by the reason that the metal catalyst in the gel mem-

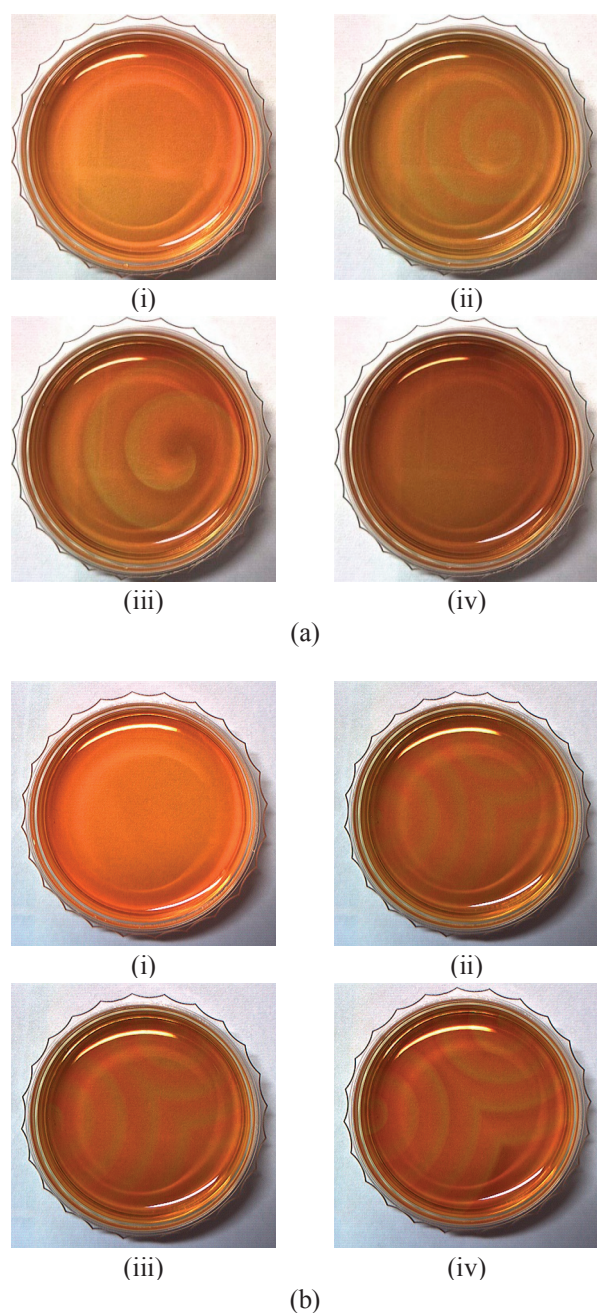


Figure 4. Propagating wave dynamics depending on $[1,4\text{-CHD}]_0$. The concentration of other reactants was fixed at a standard condition similar to Figure 2. Pattern (a) is obtained at $[1,4\text{-CHD}]_0 = 0.075$ M, $t =$ (i) 310, (ii) 350, (iii) 400, and (iv) 430 min. Pattern (b) is obtained at $[1,4\text{-CHD}]_0 = 0.05$ M, $t =$ (i) 321, (ii) 375, and (iii) 430, and (iv) 470 min, respectively. Images in (a) show typical spiral waves without folding, while images in (b) show the pattern of ripple wave.

brane system is covalently bonded in a gel network where the diffusion of reaction intermediates through the networked gel membrane may be rather slow compared to the catalyst-coated resin system. However, after 318 min the propagating waves penetrating the reduced gel membrane appear to be very clear as shown in steps (ii) - (vi). The initiation and propagation of these waves appeared in the form of a spiral where the center acts as a sink wherein incoming waves disappear. To maintain

this spiral pattern, new wave emerges at the periphery, i.e., at the boundary between the basins of two adjacent spiral waves (Figure 2. (ii) - (iv)).

Dependence of the wave on $[\text{BrO}_3^-]_0$ and $[1,4\text{-CHD}]_0$. Wave propagation of this system with a longer wavelength, clearer wave-train patterns, and longer duration period allows for a more detailed observation of wave characteristics, although it is still dependent on the reaction conditions. The concentration dependence of the patterns on $[\text{BrO}_3^-]_0$ and $[1,4\text{-CHD}]_0$ was examined within 0.125 - 0.2 M and 0.025 - 0.175 M, respectively. When $[\text{BrO}_3^-]_0$ or $[1,4\text{-CHD}]_0$ was varied, the concentrations of other reagents were fixed with the condition as used for those in Figure 2. The induction and the duration times increased with the increase in $[\text{BrO}_3^-]_0$, contrary to the case for $[1,4\text{-CHD}]_0$, which will be discussed in succeeding subsections.

Figure 3 shows the propagation dynamics of the oxidation waves obtained over the gel membrane at different $[\text{BrO}_3^-]_0$. At $[\text{BrO}_3^-]_0 = 0.125$ M as shown in Figure 3(a), the waves were similar to those in Figure 2 (0.150 M), but their appearance was neither clear nor distinct. These patterns appeared about 360 min after the start of the reaction, and culminated at about 420 min without the clear appearance of spiral patterns as shown in stages (ii) to (iv). In contrast, a well-defined pattern was observed at $[\text{BrO}_3^-]_0 = 0.175$ M as shown in Figure 3(b), where clear and concentric patterns were initiated at the bottom of the gel membrane at 408 min. Propagation of the wave changed into a spiral pattern at a later stage after 20 min from the initiation as shown in (iii). The succeeding wave of similar pattern was initiated at the core located very close to the center of the earlier waves. Furthermore, these waves coalesced and dispersed with the same velocity from initiation to disappearance. This type of wave disappeared at 470 min from the initiation as shown in stage (iv). It is well known that the velocity of ordinary BZ waves traveling in an excitable medium is proportional to $([\text{BrO}_3^-]_0)^{1/2,1,5}$. However, the dependency of wave velocity in our system does not exactly hold. The velocity is not exactly proportional to $([\text{BrO}_3^-]_0)^{1/2}$; rather, the velocity was constant as 0.2 ± 0.02 mm/min, without large change, even if the concentration changed from 0.125 M to 0.175 M. Compared to the excitable system using the catalyst immobilized resin system, the propagating velocity is very low.²⁷ This can be interpreted by the fact that the kinetics of redox reaction are perturbed and therefore physical diffusion phenomenon has a significant role in the formation of the traveling wave in the gel membrane system, wherein the linear relationship between the velocity of the waves and $([\text{BrO}_3^-]_0)^{1/2}$ could not hold.

Figure 4 shows the dependence of wave patterns on the concentration of $[1,4\text{-CHD}]_0$ at the conditions where the other parameters were kept constant. Figure 4(a) shows a traveling wave obtained by the condition $[1,4\text{-CHD}]_0 = 0.075$ M. Differently from the folded spiral wave shown in Figure 2, stage (i) shows a typical evolution of a spiral pattern with a longer wavelength from one initiating core. The wave succeeded continuously with the same patterns as shown in stage (ii). These waves disappeared at the same point where the initiation occurred as shown in stage (iii). Figure 4(b) shows the behavior of the waves at $[1,4\text{-CHD}]_0 = 0.05$ M. At this low concentration of $[1,4\text{-CHD}]_0$, the initiation occurred at the periphery region of the gel at 375 min

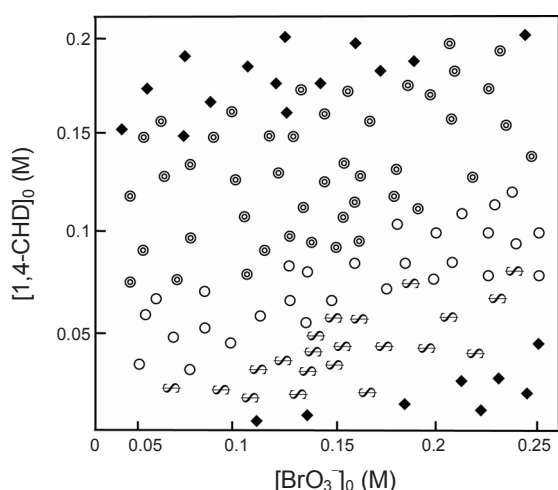


Figure 5. Phase diagram of the wave dynamics on the $[\text{BrO}_3^-]_0$ - $[1,4\text{-CHD}]_0$ plane, showing a folding spiral wave shown in Figure 2 (●), spiral pattern with a longer wavelength with one initiating core as shown in Figure 4(a) (○), concentric and ripple wave propagation shown in Figure 3(b) and 4(b) (⊄), and no-wave formation region (◆).

as shown in the stage (ii) with a ripple pattern and the wave slowly propagated along the medium without the formation of a concentric pattern. This ripple wave is completely different in wave pattern propagation compared to those in Figures 2, 3(a) and 4(a), wherein an initiation core for the spiral wave formation exists. Thus, the circular wave initiated at the periphery of the catalyst gel spread outward to become a ripple wave. And newly generated propagating waves coalesced until it sufficiently consumed of 1,4-CHD. Upon comparison of the propagating wave patterns of Figure 4(a) and 4(b), we can easily see that the front part's initiation and propagation is governed so much by the initial concentration of 1,4-CHD.

Variations in $[\text{BrO}_3^-]_0$ and $[1,4\text{-CHD}]_0$ caused different wave patterns. In any of these cases, the redox profile of the catalyst distributed in space formed target patterns. The oxidation wave began to propagate outwards through the reduced medium. After a certain time the second wave originated at the leading center followed the first wave.

The waves obtained at different $[\text{BrO}_3^-]_0$ and $[1,4\text{-CHD}]_0$ in the present system show patterns depending on the reaction condition, with a longer wavelength, clearer wave-train patterns, and longer duration period. The oscillatory period decreased with increasing $[\text{BrO}_3^-]_0$, and increased along with an increasing $[1,4\text{-CHD}]_0$. The induction time increased with increasing $[\text{BrO}_3^-]_0$, but decreased with increasing $[1,4\text{-CHD}]_0$. By increasing $[1,4\text{-CHD}]_0$, the spiral wave was generated from the center or the peripheral region.

Phase diagram on $[\text{BrO}_3^-]_0$ - $[1,4\text{-CHD}]_0$. Figure 5 shows the phase diagram of the wave dynamics in the $[\text{BrO}_3^-]_0$ - $[1,4\text{-CHD}]_0$ plane, which can be roughly divided into four regions: the folding-spiral waves propagating into inside from outwards (Figure 2); spiral waves with large wave length by a single initiating core (Figure. 4(a)); ripple waves with concentric propagation (Figure 4(b)); and the absence of wave formation. The phase diagram clearly shows that the wave types obtained in

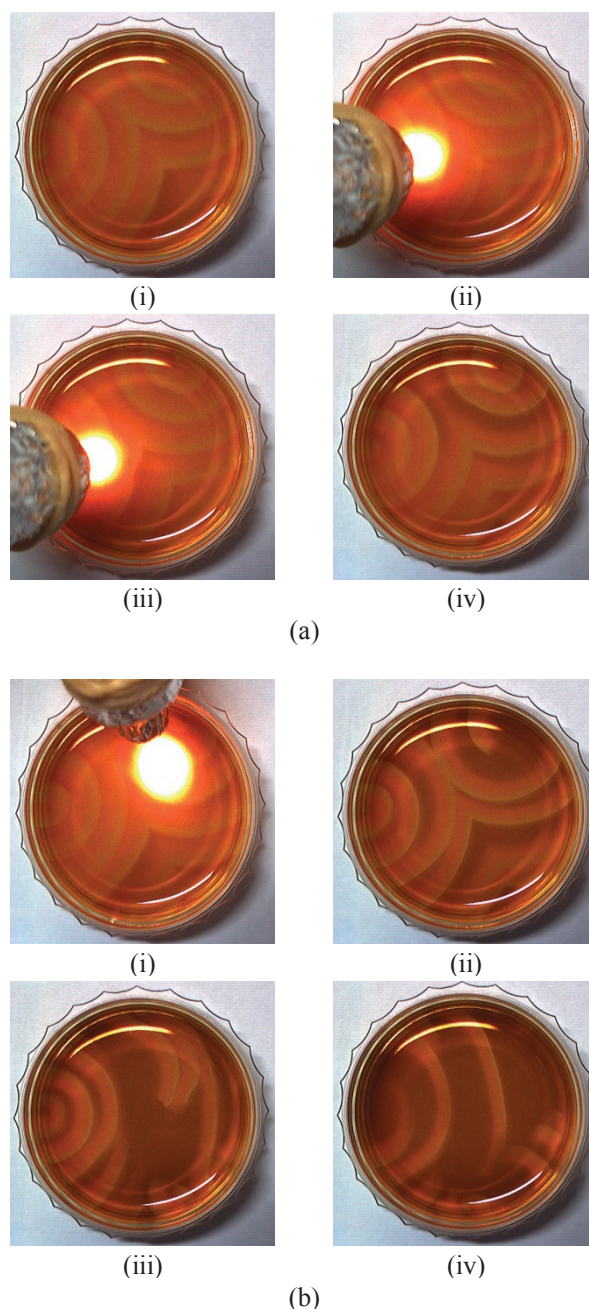


Figure 6. The effect of illumination of visible light on the wave propagation in a gel membrane depending on the intensity of the illumination at $[\text{BrO}_3^-]_0 = 0.15 \text{ M}$, $[\text{H}^+]_0 = 1.0 \text{ M}$, $[1,4\text{-CHD}]_0 = 0.05 \text{ M}$, and $[\text{Ru}(\text{bpy})_3^{2+}]_0 = 1.75 \text{ mM}$. Pattern (a) shows the images obtained at the intensity of illumination of 15 mW^{-2} . Image (i) shows the behavior right before illumination, images (ii) and (iii) show the state during the illumination with 60 s. Image (iv) shows the image 5 min after the end of illumination. Pattern (b) shows the images obtained at the intensity of the light illumination of 40 mW^{-2} . Image (i) shows the perturbation by the single pulse light for 60 s. Images (ii) are recorded at 5 min after the illumination. Image (iii) and (iv) show the state recorded at 20 and 40 after the illumination, respectively.

this system depends greatly on $[1,4\text{-CHD}]_0$ as shown in the diagram. In the regions lower than a critical concentration of $[1,4\text{-CHD}]_0$, a spiral pattern was not obtained, rather a concentric

ripple wave propagating outward was formed. Thus, the waves changed their phases across the bifurcation lines on the $[1,4\text{-CHD}]_0 - [\text{BrO}_3^-]_0$ plane. The decrease in the concentration of the chemicals in accordance with the progress of the BZ reaction changes the morphology of transient waves by splitting into diverse spiral waves. Beyond the critical concentrations, no waves appeared in the system.

The effect of visible light illumination on the waves in the gel membrane system. Figure 6 presents a series of snapshots showing the photosensitivity of the waves in the gel membrane system depending on the intensity of the illuminating light. The intensity of light applied was 15 mW cm^{-2} and 40 mW cm^{-2} for Figure 6(a) and 6(b), respectively. The initial compositions of the reaction solution were $[1,4\text{-CHD}]_0 = 0.05 \text{ M}$, $[\text{BrO}_3^-]_0 = 0.15 \text{ M}$, and $[\text{H}^+]_0 = 1.0 \text{ M}$, which correspond to the condition that induce ripple wave as shown in Figure 4(b). A single pulse illumination with a moderate intensity as 15 mW cm^{-2} , which lasted for 60 s, did not cause a modulation of the wave pattern as shown in stage (ii) in Figure 6(a). However, succeeding illumination with additional 60 s deformed a little the propagating pattern as shown in stage (iii). However, the propagating wave was rapidly recovered into its original state when the illumination was stopped, as shown in stage (iv), similar to the pattern of stage (i) prior to illumination. However, when a stronger illumination of 40 mW cm^{-2} was applied to the gel membrane system, wave propagation became greatly affected by illumination as shown in Figure 6(b). After the perturbation by the single pulse illumination for 60 s (stage (i)), a clear disturbance by the illumination, in which the propagation of wave is broken simultaneously with the initiation of a spiral pattern as shown in stage (ii). Stages (iii) and (iv) clearly show the change of wave pattern from their original propagation prior to illumination; this brought out a rapid disappearance of the wave as shown in stage (iv). Similarly, we can easily see that the illumination of a visible light by a stronger illumination induces a deep shadow in front of the wave propagation like as a 3-D pattern. This may have been caused by the thickness of the gel membrane.

Conclusion

In this study, we observed the complex spiral waves appearing in the reaction system wherein the poly(AAm-co-Ru(bpy)₃²⁺) gel membrane was used as a metal catalyst for the BZ reaction. The patterns basically depended on $[\text{BrO}_3^-]_0$ and $[1,4\text{-CHD}]_0$, which is evidenced in the variation of wave patterns caused by the initial conditions of the reaction system. Our experimental results suggest that a kind of gel membrane where the metal catalyst is covalently immobilized provides a superior reaction medium for the RD pattern formation in the BZ type reaction system. This may be a result of the eliminated disturbance in wave propagation induced from the secession of the immobilized metal catalyst into a highly acidic solution since the metal catalyst is covalently bonded in the gel membrane network. Obviously, there is a great difference in the pattern formation between in the membrane and in the discrete beads medium comprising an initiating point for triggering a new wave. And differently from the ordinary BZ waves traveling in an excitable medium, the velocity was not proportional to

$([\text{BrO}_3^-]_0)^{1/2}$. The dependency of wave velocity in our system does not exactly hold, rather the velocity was constant as $0.2 \pm 0.02 \text{ mm/min}$ without large change by varying the concentration of BrO_3^- .

Based on our studies on the effect of visible light illumination, we found that wave propagation was greatly photosensitive to intense illumination. Stronger illumination greatly modulated the pattern of wave propagation and eliminated wave activity; these results are similar to those of Kurin-Csörgei *et al.*²³ in the ferroin-immobilized resin system using a modified BZ system with 1,4-CHD. The weak photosensitivity of the wave pattern in this gel system may be due to the metal catalyst being covalently bonded through the cross-linking present in the gel network. However, continuous studies are on progress in our group to uncover the effect of illumination in more detail.

References

- Kapral, R., Showalter, K., Eds.; *Chemical Waves and Patterns*; Kluwer Academic Publishers: Netherlands, 1995.
- Cross, M. C.; Hohenberg, P. C. *Rev. Mod. Phys.* **1993**, *65*, 851.
- Swinney, H. L., Krinsky, V. I., Eds.; *Physica D*; 1991; Vol. 49.
- Winfree, A. T. *The Geometry of Biological Time*; Springer: Heidelberg, 2000.
- Field, R. J., Burger, M., Eds.; *Oscillations and Traveling Waves in Chemical Systems*; Wiley-Interscience: New York, 1985.
- Agladze, K.; Thouvenel-Romans, S.; Steinbock, O. *J. Phys. Chem. A* **2001**, *105*, 7356.
- Bertram, M.; Masere, J.; Pojman, J. A.; Volke, F. *Polym. Sci. A* **2001**, *39*, 1075.
- Hohnson, A.; Brighm, E. S.; Oliver, P. J.; Moluk, T. E. *Chem. Mater.* **1997**, *9*, 2448.
- Schluter, A. D., Ed.; *Materials Synthesis and Technology, A Comprehensive Treatment*; Wiley-VCH: Weinheim, New York, 1999.
- Orlandini, E.; Stella, A. L.; Vanderzande, C. V. *J. Stat. Phys.* **2004**, *115*, 681.
- Persijn, J. P.; Van Duijn, P. *Histochemistry and Cell Biology* **1961**, *2*, 283.
- Bensemman, I. T.; Fialkowski, M.; Grzybowski, B. A. *J. Phys. Chem. B* **2005**, *109*, 2774.
- Bishop, K. J. M.; Fialkowski, M.; Grzybowski, B. A. *J. Am. Chem. Soc.* **2005**, *127*, 15943.
- Huh, D. S.; Choe, S. J.; Kim, M. S. *React. Kinet. Catal. Lett.* **2001**, *74*, 11.
- Wang, J.; Yadav, K.; Zhao, B.; Gao, Q. A.; Huh, D. S. *J. Chem. Phys.* **2004**, *10138*, 121.
- Bansagi, T.; Palczewski, J. C.; Steinbock, O. *J. Phys. Chem. A* **2007**, *111*, 2492.
- Klug, J. *J. Mol. Biol.* **2004**, *335*, 2.
- Yoshida, R.; Kokufuta, E.; Yamaguchi, T. *J. Am. Chem. Soc.* **1996**, *118*, 5234.
- Vanag, V. K. *Physica-Uspeski*. **2004**, *47*, 923.
- Maselko, J.; Reckley, J. S.; Showalter, K. *J. Phys. Chem.* **1989**, *93*, 2774.
- Yoshikawa, K.; Aihara, R.; Agladze, K. *Phys. Chem.* **1989**, *102*, 7649.
- Kurin-Csörgei, K.; Körös, E. *Kinet. Catal. Lett.* **1995**, *54*, 217.
- Kurin-Csörgei, K.; Zhabotinsky, A. M.; Orban, M.; Epstein, I. R. *J. Phys. Chem. A* **1997**, *101*, 6827.
- Kurin-Csörgei, K.; Zhabotinsky, A. M.; Orban, M.; Epstein, I. R. *J. Phys. Chem.* **1996**, *100*, 5393.
- Kurin-Csörgei, K.; Szalai, I.; Molnár-Perl, I.; Körös, E. *Kinet. Catal. Lett.* **1994**, *53*, 115.
- Szalai, I.; Körös, E. *J. Phys. Chem. A* **1998**, *102*, 6892.
- Huh, D. S.; Kim, Y. J.; Kim, H. S.; Kang, J. K.; Wang, J. *Phys. Chem.*

- Chem. Phys.* **2003**, *5*, 3188.
28. Panfilov, A. V. *Chaos* **1998**, *8*, 57.
29. Tanaka, T. *Phys. Rev. Lett.* **1978**, *40*, 820.
30. Hirokawa, Y.; Tanaka, T. *J. Chem. Phys.* **1981**, *81*, 6379.
31. Kawasaki, H.; Sasaki, S.; Maeda, H. *J. Chem. Phys.* **1997**, *101*, 5089.
32. Tanaka, T.; Nishio, I.; Sun, S. T.; Ueno-Nishio, S. *Science* **1982**, *218*, 467.
33. Schild, H. G. *Prog. Polym. Sci.* **1992**, *17*, 163.
34. Yoshida, R.; Uchida, K.; Kaneko, Y.; Sakai, K.; Kikuchi, A.; Sakurai, Y.; Okano, T. *Nature* **1995**, *374*, 240.
35. Yoshida, R.; Takahashi, T.; Yamaguchi, T.; Ichijo, H. *J. Am. Chem. Soc.* **1996**, *118*, 5234.
36. Yoshida, R.; Kokufuta, E.; Yamaguchi, T. *Chaos* **1999**, *9*, 260.
37. Yoshida, R.; Takahashi, T.; Yamaguchi, T.; Ichijo, H. *Adv. Mater.* **1997**, *9*, 175.
38. Kaern, M.; Menzinger, M.; Hunding, A. *Biophys. Chem.* **2000**, *87*, 121.
39. Petrov, V.; Ouyang, Q.; Swinney, H. L. *Nature* **1997**, *388*, 655.
40. Vanag, V. K.; Yang, L.; Dolnik, M.; Zhabotinsky, A. M.; Epstein, I. R. *Nature* **2000**, *406*, 389.
41. Vanag, V. K.; Zhabotinsky, A. M.; Epstein, I. R. *Phys. Rev. Lett.* **2001**, *86*, 552.
42. Wang, J.; Kádár, S.; Jung, P.; Showalter, K. *Phys. Rev. Lett.* **1999**, *82*, 855.
43. Kádár, S.; Wang, J.; Showalter, K. *Nature* **1998**, *391*, 770.
44. Kuhnert, L.; Agladze, K. I.; Krinsky, V. I. *Nature* **1989**, *337*, 244.
45. Steinbock, O.; Zykov, V. S.; Müller, S. C. *Nature* **1993**, *366*, 322.
-